

# Symmetry, shape and order

Antonio Trovato,<sup>1,2</sup> Trinh X. Hoang,<sup>3,4</sup> Jayanth R. Banavar,<sup>4</sup> and Amos Maritan<sup>1,2,5</sup>

<sup>1</sup>*Dipartimento di Fisica ‘G. Galilei’, Università di Padova,*

*Via Marzolo 8, I-35131 Padova, Italy*

<sup>2</sup>*CNISM, Unità di Padova, Via Marzolo 8, I-35131 Padova, Italy*

<sup>3</sup>*Institute of Physics and Electronics,*

*Vietnamese Academy of Science and Technology, 10 Dao Tan, Hanoi, Vietnam*

<sup>4</sup>*Department of Physics, 104 Davey Laboratory,*

*The Pennsylvania State University,*

*University Park, Pennsylvania 16802*

<sup>5</sup>*Sezione INFN, Università di Padova, I-35131 Padova, Italy*

## Abstract

Packing problems have been of great interest in many diverse contexts for many centuries. The optimal packing of identical objects has been often invoked to understand the nature of low temperature phases of matter. In celebrated work, Kepler conjectured that the densest packing of spheres is realized by stacking variants of the face-centered cubic lattice and has a packing fraction of  $\pi/(3\sqrt{2}) \sim 0.7405$ . Much more recently, an unusually high density packing of approximately 0.770732 was achieved for congruent ellipsoids. Such studies are relevant for understanding the structure of crystals, glasses, the storage and jamming of granular materials, ceramics, and the assembly of viral capsid structures. Here we carry out analytical studies of the stacking of close-packed planar layers of systems made up of truncated cones possessing uniaxial symmetry. We present examples of high density packing whose order is characterized by a *broken symmetry* arising from the shape of the constituent objects. We find a biaxial arrangement of solid cones with a packing fraction of  $\pi/4$ . For truncated cones, there are two distinct regimes, characterized by different packing arrangements, depending on the ratio  $c$  of the base radii of the truncated cones with a transition at  $c^* = \sqrt{2} - 1$ .

## I. INTRODUCTION

Many natural forms [1], such as the DNA double helix [2, 3] and seed arrays on sunflowers [4], arise from simple geometrical principles rather than from complex interactions. Symmetry considerations often play a key role in determining the nature of order of a system [5, 6]. The simplest model of matter, a collection of isotropic objects (spheres) exhibits both the isotropic fluid and the crystalline phases with a phase transition between them on varying the packing fraction or density [7]. Dense packing can result from either the maximization of the packing fraction [7] or from the minimization of the area exposed [8, 9] to probe objects such as water molecules. Efficient packing of a system of rods [10] leads again to an isotropic fluid phase or to uniaxial order with the orientation of the axis of one of the rods dictating the preferred alignment of nearby rods. Liquid crystalline phases [5] exist between a liquid with no translational order and a crystal with translational order in all three directions. This is accomplished by employing constituent particles which are anisotropic – the molecules of liquid crystals are not spherical and can form phases with translational order in fewer than three dimensions and/or orientational order. Recent work has shown that an unusually high density packing of approximately 0.770732 is achieved for congruent ellipsoids [11]. Packing studies are relevant for understanding the structure of crystals, glasses, the storage and jamming of granular materials and ceramics [12, 13, 14, 15, 16, 17, 18].

Here we study the packing of truncated cones and show how the nature of order of a system composed of identical objects can depend not only on the symmetry of the object but also on its shape. The geometry of small self-assembled clusters of cones has been studied in the context of the geometry of viral capsids [19]. The packing of cones has also been shown to be relevant for understanding the geometry of amphiphile nanoparticles having a hydrophobic tail and a hydrophilic head [20]. Tightly packed hierarchical arrangements are obtained by first aggregating the cones into spheres or cylinders and then packing these in a face-centered-cubic lattice or a hexagonal Abrikosov flux lattice [5] respectively. We will instead first arrange cones within close-packed planar layers and then stack different layers on top of each other. We begin with a discussion of the packing of solid cones and then study the more general case of the dense packing of solid truncated cones.

## II. RESULTS AND DISCUSSION

### A. Cone packing

There are three natural close-packed geometries (Figure 1) of a pair of cones. The space-filling arrangements of the cones shown in Figs. 1(d) and 1(e) are effectively two dimensional with biaxial order arising from the breaking of the uniaxial symmetry of the cone in order to achieve close packing \*. A collection of bicones (Figs. 1(d) and 1(e)) or hour glasses (Fig. 1(d)) can also exhibit biaxial order. There are other high density arrangements of cones obtained by first assembling them into basic units and densely packing these units. Figs. 1(f) and 1(g) depict a helical assembly. Fig. 2 shows a stack of planes with cones arranged as in Figs. 1(d).

We will assume that the cones have flat bases with the opening angle  $\alpha$  at their apex and the slant height  $L$ . In micelles [20], the solvent induces a tip-to-tip attraction between the cones. Here we consider the role of base-to-base stacking in facilitating planar packing. The cone volume is given by  $V_{cone} = \pi L^3 \sin \alpha \sin \left( \frac{\alpha}{2} \right) / 6$ . For the stack of planes shown in Fig. 2, the volume of a elementary cell is equal to

$$V_{cell}^{pl} = h \cdot d \cdot s = \frac{2}{3} L^3 \sin(\alpha) \sin \left( \frac{\alpha}{2} \right), \quad (1)$$

where  $h$ ,  $d$  and  $s$  are the dimensions of the cell as described in Fig. 2. Thus, the packing fraction of the cones in this case is equal to

$$F = \frac{V_{cone}}{V_{cell}^{pl}} = \frac{\pi}{4}, \quad (2)$$

which is independent of  $\alpha$ .

Interestingly, there is an infinite degeneracy in the close-packing arrangements of cones stacked in planar layers as in Fig. 2(b), due to the possibility of choosing between positive and negative shifts each time a new layer is added to the stack. This is reminiscent of the

---

\* The arrangement of discrete cylinders stacked in an Abrikosov lattice is not isotropic in the plane perpendicular to the cylinder axis – rather, it is invariant under discrete rotations (by integer multiples of  $\pi/3$ ) with three equivalent directions. We will, anyhow, denote as uniaxial arrangements possessing at least two equivalent directions within the plane perpendicular to the symmetry axis. Biaxial order is one in which a privileged direction exists in that plane so that the only residual symmetry is the invariance under rotations by  $\pi$  [5]. This broken symmetry arises from the shape of the constituent objects, even though they are uniaxial.

two-fold stacking choice made at each hexagonal layer in the random hexagonal close packed structure of spheres leading to the stacking variants of the face-centered cubic lattice which share Kepler's optimal packing fraction (0.7405) [5]. Remarkably, the packing fraction of identical cones,  $F \sim 0.78539$ , is higher than the latter, in accord with the suggestion that spheres cannot be packed as efficiently as other convex objects [19]. The packing fraction of cones is also higher than the maximum packing fraction recently found for dense crystal packing of ellipsoids (0.770732) [11].

It is interesting to compare the packing fraction of this biaxial arrangement with the common assemblies of amphiphile nanoparticles [20]: the spherical micelles in a face-centered-cubic lattice arrangement and the hexagonal arrangement of cylindrical micelles. Note that a definitive proof of the most tightly packed arrangement is highly non-trivial. For the simpler case of the packing of spheres, Kepler's conjecture was finally proved only within the last decade [7]. For a spherical micelle, as shown by Tsonchev et al. [20], the number of cones in each sphere is given by  $N_s = \left\lfloor \frac{2\pi}{3\gamma - \pi} \right\rfloor$ , where  $[x]$  denotes the integer part of  $x$  and  $\gamma = \arccos\left(\frac{\cos(\alpha)}{2\cos^2(\alpha/2)}\right)$  for small enough  $\alpha$  such that the cones (or cone bases) form a hexagonal arrangement in the sphere surface. This assumption is certainly valid when  $\alpha \leq \pi/3$  ( $N_s = 11$  for  $\alpha = \pi/3$ ).  $N_s = 3$  for  $\alpha \rightarrow 2\pi/3$  from below and equal to 2 for  $\alpha$  larger than  $2\pi/3$ . The packing fraction of spheres in a face-centered-cubic lattice arrangement is  $\pi/(3\sqrt{2})$  [5]. One therefore finds that the packing fraction of cones in spherical micelles is given by

$$F_{sph} = \frac{\pi}{24\sqrt{2}} \sin(\alpha) \sin\left(\frac{\alpha}{2}\right) N_s. \quad (3)$$

For a cylindrical micelle, the number of cones in an elementary cell, defined as a cylinder section of thickness  $L \sin(\alpha/2)\sqrt{3}/2$  [20], is  $N_c = \left\lfloor \frac{2\pi}{\alpha} \right\rfloor$  and the volume of such an elementary cell is  $V_{cell}^{cyl} = \pi L^3 \sin(\alpha/2)\sqrt{3}$ . The packing fraction of cylinders in a hexagonal arrangement is  $\pi/(2\sqrt{3})$ . Thus a hexagonal arrangement of cylindrical micelles formed by flat-based cones yields a packing fraction of

$$F_{cyl} = \frac{\pi}{36} \sin(\alpha) \left\lfloor \frac{2\pi}{\alpha} \right\rfloor. \quad (4)$$

Fig. 3 shows that the biaxial arrangements lead to a denser packing than both the hexagonal arrangement of cylindrical micelles [20] and the spherical micelle [20] in a face-centered-cubic lattice arrangement. Note that the use of cones with curved bases improves the packing fraction of both cylindrical and spherical micelles [20].

## B. Truncated cone packing

We turn now to the more general case of the packing of truncated cones (conical frustum) shown in Fig. 4 which provides a natural bridge between a cylinder ( $a = b$ ) and a cone ( $b = 0$ ).

Following our previous analysis, we arrange the objects in a close-packed planar layer, as in Fig. 5, and then stack consecutive layers on top of each other. A reference frame is attached to each layer, as in Fig. 5, so that the shift between consecutive layers is characterized by  $(\Delta x, \Delta y, \Delta z)$ , the relative displacement of the two origins. We do not consider rotations (along the  $z$  axis) because they generally lead to a worse packing. Our goal then is to accomplish close packing by minimizing  $\Delta z$  through the appropriate selection of  $\Delta x$  and  $\Delta y$ . It is crucial to consider the circles cut out by intersecting the plane  $y = 0$  with successive cone layers in the stacking (see Fig. 6). The condition of mutual tangency of three such circles determines the minimum distance between successive layers (see Supplementary Material for details).

In general, one finds two different degenerate (i.e. yielding the same minimum  $\Delta z$ ) solutions: one for  $r < R$  and the other for  $r > R$ . They can be thought of as being related by a mirror symmetry  $x \rightarrow -x; y \rightarrow -y$  applied to the second layer while keeping the first layer fixed (see Supplementary Material for details). Note that this choice among two possibilities exists each time a new layer is added to the stack yielding an infinite degeneracy in the close-packing arrangements of cones stacked in planar layers. Upon choosing symmetrically staggered layers, the center of the circles cut out in the  $y = 0$  plane arrange themselves on a regular planar lattice. The symmetry displayed in the latter (and in the corresponding triangular tiling of the plane  $y = 0$  obtained by joining the circle centers) is related to the uniaxiality/biaxiality of the corresponding packing arrangement.

Remarkably, the optimal stacking and the related symmetries depend on the value of the ratio  $c = b/a$  with a transition point at  $c^* = \sqrt{2} - 1$  separating two distinct classes of behavior (see Methods for a detailed discussion of symmetries and packing fraction equations in the different regimes). The special case of a cylinder,  $c = 1$ , characterized by the hexagonal Abrikosov lattice, yields a tiling of equilateral triangles. In the cylinder-like regime,  $1 > c > c^*$ , isosceles triangles form a rhombic lattice (see Fig. 7), whereas in the cone-like regime,  $0 \leq c < c^*$ , right angled triangles result in a rectangular lattice (see Fig. 8). At

the transition point between the two regimes,  $c = c^*$ , right angled isosceles triangles result in a square lattice (see Fig. 9). Cylinders ( $c = 1$ ) and truncated cones at the transition point ( $c = c^*$ ) are special cases where uniaxiality is maintained since different directions are equivalent in the plane orthogonal to their axes. In all other cases ( $1 > c > c^*$  and  $0 \leq c < c^*$ ) no such symmetry is present, implying biaxial order.

Fig. 10 shows a plot of the packing fraction  $f(c)$  as a function of the base radii ratio  $c = b/a$  from Equations (5) and (6). The transition at  $c = c^*$  between the cone-like and the cylinder-like regimes is clearly visible. Most notably, the packing fraction does not increase monotonically with  $c$  in either regime so that both the transition point ( $c = c^*$ ) and the cone point ( $c = 0$ ) are local maxima for the packing fraction.

### III. CONCLUSIONS

Truncated cones are inherently uniaxial objects. Since they smoothly interpolate between cylinders and cones we were able to assess the relevance of shape in dictating the nature of the packing. The rigorous determination of the optimal packing is a formidable problem and the well-packed arrangements we have found can at best be thought of as conjectures of the best optimal packing. The packings we have investigated are all based on the simplifying hypothesis that the optimal solutions are formed from the assembly (stacking) of close-packed planar layers. Within this assumption, we have shown that the optimal packing of uniaxial truncated cones is characterized by broken symmetry and is in general biaxial with the exception of the (degenerate) cylindrical case and of a special value of the 'aspect ratio'  $c^* = \sqrt{2} - 1$ . We have shown that the tiling of the truncated cone cross-section in the plane orthogonal to their axes is a useful way to understand the nature of the order, allowing one to distinguish between two different regimes,  $c > c^*$  and  $c < c^*$ . At the transition point separating the two regimes, truncated cones with  $c^* = \sqrt{2} - 1$  have interesting symmetry properties. The packing fraction that is achieved by truncated cones is remarkably high.

We conclude with a speculation pertaining to the building blocks of protein native state structures – uniaxial helices and biaxial sheet. There is a simple way of understanding how helices can emerge as a natural compact form adopted by a uniaxial tube. There is

no equally simple way of rationalizing the existence of zig-zag strands which assemble into almost planar, biaxial sheets. Our results above suggest that even uniaxial objects, because of their shape, can exhibit broken symmetry and biaxial order. Instead of thinking of the packing of separate objects, consider now the case of a linear chain molecule made up of objects tethered together. There is a special axis at any location along the chain defined by the positions of the adjoining tethered objects. This leads naturally to the requirement that the constituent objects at least have uniaxial symmetry rather than be isotropic objects or spheres. Such a chain of anisotropic coins can be thought of as having a tube-like geometry in the continuum limit. The helix is a natural compact arrangement of a flexible tube and strikingly a tightly wound space-filling helix has the same pitch-to-radius ratio as  $\alpha$ -helices in proteins, which are relatively short polymer chains [21]. Figs. 1(f) and 1(g) depict a helical confirmation [22] of a short chain of bicones (Fig. 1(h)). Fig. 1(d) shows an alternate well packed conformation of the chain. Such biaxial, planar sheet-like structures [23] are employed by nature not only in the amyloidin structure [24, 25] of proteins but also as a building block, along with the helix, of protein native state structures. Furthermore, there is a coordinated positioning of the amino acid side chains perpendicular to the plane of the sheet. The simple calculations we have presented here illustrate how, in principle, both the uniaxial helix and the biaxial sheets can emerge as the anisotropic building blocks of protein structures.

#### IV. METHODS

The minimum  $\Delta z$  obtained on stacking two planar layers determines the packing fraction  $F = V_{tc}/V_{\text{cell}}$  where  $V_{\text{cell}} = h\Delta z (a + b)$  is the volume of the elementary cell in the periodic arrangement of truncated cones and  $V_{tc} = (\pi h/3) (a^2 + ab + b^2)$  is the volume of the truncated cone. Different regimes are found depending on the value of  $c$ . More details are given in Supplementary Material.

##### 1. *Cylinder-like regime: $c > c^*$*

The packing fraction is

$$F = \frac{\pi}{6} \frac{1 + c + 1/c}{\sqrt{1 + 2/c}}. \quad (5)$$

The triangle obtained on connecting the centers of the three circles involved in the mutual tangency condition (see Fig. 6) is isosceles, since two of the circles have the same radius ( $r = a$  or  $r = b$ ). Note that for these solutions the only effective mirror symmetry is  $x \rightarrow -x$ , because  $\Delta y = h$  or  $\Delta y = 0$ .

For the limiting case of a cylinder ( $a = b$ ) we correctly obtain  $\frac{\pi}{2\sqrt{3}} = 0.9069\dots$  and the triangle defined above becomes equilateral. The restoration of uniaxiality in this limit is underscored by the invariance of the resulting triangular tiling of the  $(x, z)$  plane, under rotation by an integer multiple of  $\pm 60^\circ$ .

The breaking of the uniaxial symmetry occurs as soon as  $b$  is strictly smaller than  $a$  and it is accompanied by: i) all the triangles becoming isosceles and ii) only half of them being associated with the mutual tangency condition (see Fig. 7) yielding the two-fold degeneracy discussed above. Note that on moving along the  $y$  axis, the circles formed in the  $(x, z)$  plane change their radii.

## 2. Cone-like regime: $c < c^*$

The packing fraction is

$$F = \frac{\pi}{6} \frac{(3 + c)(1 + c + 1/c)}{(1 + c)(1 + 2/c)}. \quad (6)$$

Note that for these solutions the only effective mirror symmetry is  $y \rightarrow -y$ , because  $\Delta x = a + b$  or  $\Delta x = 0$  (see Figs. 8 and 11).

In the limiting case of a regular cone ( $b = 0$ ) we correctly obtain  $F = \frac{\pi}{4} = 0.7854\dots$

The triangles defined above are always right angled but never isosceles. The triangular tiling of the  $(x, z)$  plane thus results in a rectangular tiling. Again, only half of the triangles are associated with the mutual tangency condition (see Fig. 8) and uniaxial symmetry is broken (i.e. no rotation symmetry is present in the plane).



### 3. Transition point: $c = c^*$

The special value  $c = c^*$ , i.e.  $b = (\sqrt{2} - 1)a$ , separates the two above regimes. At  $c = c^*$  the packing fraction is

$$F = \frac{\pi}{6} (3 - \sqrt{2}) = 0.8303\dots \quad (7)$$

The triangles defined above are isosceles right angled and the degeneracy disappears. Indeed the two degenerate solutions merge one into the other and one obtains a square tiling in the  $(x, z)$  plane (see Fig. 9). Uniaxiality is restored in this special case because the square tiling is invariant under rotation by an integer multiple of  $\pm 90^\circ$ . The triangles are no longer isosceles and the square tiling become rectangular for any  $c < c^*$  (see Fig. 8), whereas the triangles are no longer right angled for any  $c > c^*$  (see Fig. 7).

### Acknowledgments

This work was supported by PRIN no. 2005027330 in 2005, INFN, the NSC of Vietnam, and the Vietnam Education Foundation.

- 
- [1] Thompson DW (1942) *On growth and form* (Cambridge University Press, Cambridge).
  - [2] Pieranski P (1998) in *Ideal Knots*, eds Stasiak A, Katritch V, Kauffman LH (World Scientific, Singapore), pp 20-41.
  - [3] Stasiak A, Maddocks JH (2000) *Nature* 406:251-253.
  - [4] Klar AJS (2002) *Nature* 417:595-595.
  - [5] Chaikin PM, Lubensky TC (2000) *Principles of condensed matter physics* (Cambridge University Press, Cambridge).
  - [6] Penrose tilings and quasicrystals are space filling and apparently regular but non-periodic arrangements arising from mixing tiles with different symmetries. See, e.g., (1991) *Quasicrystals: The State of the Art*, eds DiVincenzo DP, Steinhardt PJ (World Scientific, Singapore).
  - [7] Szpiro GG (2003) *Kepler's conjecture* (John Wiley, New York).
  - [8] Chandler D (2005) *Nature* 437:640-647.

- [9] Banavar JR, Hoang TX, Maddocks JH, Maritan A, Poletto C, Stasiak A, Trovato A (2007) *Proc Natl Acad Sci USA* accepted for publication.
- [10] Onsager L (1949) *Ann NY Acad Sci* 51:627-659.
- [11] Donev A, Stillinger FH, Chaikin PM, Torquato S (2004) *Phys Rev Lett* 92: 255506.
- [12] Aste T, Weaire D (2000) *The Pursuit of Perfect Packing* (IOP, London).
- [13] Chaikin PM (2000) in *Soft and Fragile Matter, Nonequilibrium Dynamics, Metastability and Flow*, eds Cates ME, Evans MR (Institute of Physics, London), pp 315-348.
- [14] Conway JH, Sloane NJA (1999) *Sphere Packings, Lattices, and Groups, Ed. 3* (Springer-Verlag, New York).
- [15] Edwards SF (1994) in *Granular Matter*, ed Mehta A (Springer-Verlag, New York), pp 121-140.
- [16] Liu AJ, Nagel SR (1998) *Nature* 396:21-22.
- [17] Makse HA, Kurchan J (2002) *Nature* 415:614-617.
- [18] Zallen R (1983) *The Physics of Amorphous Solids* (Wiley, New York).
- [19] Chen T, Zhang Z, Glotzer SC (2007) *Proc Natl Acad Sci USA* 104:717-722.
- [20] Tsonchev S, Schatz, GC, Ratner MA (2003) *Nano Lett* 3:623-626.
- [21] Maritan A, Micheletti C, Trovato A, Banavar JR (2000) *Nature* 406:287-290.
- [22] Pauling L, Corey RB, Branson HR (1951) *Proc Natl Acad Sci USA* 37:205-211.
- [23] Pauling L, Corey RB (1951) *Proc Natl Acad Sci USA* 37:729-740.
- [24] Fowler DM, Koulov AV, Alory-Jost C, Marks MS, Balch WE, Kelly JW (2006) *PLOS Biol* 4:100-107.
- [25] Dobson CM (2003) *Nat Rev Drug Discov* 2:154-160.

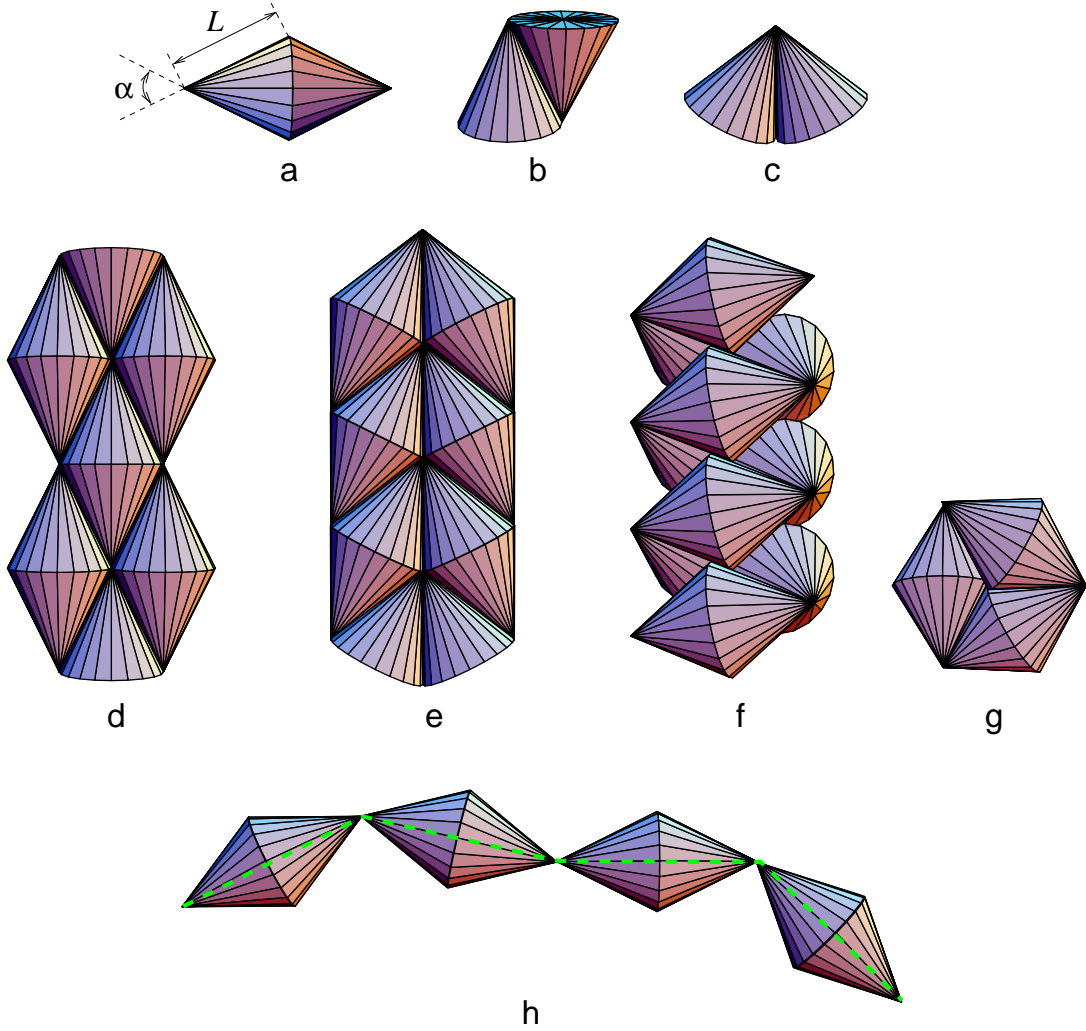


FIG. 1: Three close-packed configurations of two identical cones: a) the cones form a bicone, b) the cones point in opposite directions, and c) the cones axes are not parallel. d) and e) Two close-packed configurations of many identical cones. Note that both arrangements are necessarily planar to achieve close packing. f) and g) Two views of a close-packed helix, a common motif in biomolecular structure h) A linear chain made of 4 identical bicones. Configurations (d), (f) and (g) are viable close-packed arrangements for a chain molecule.

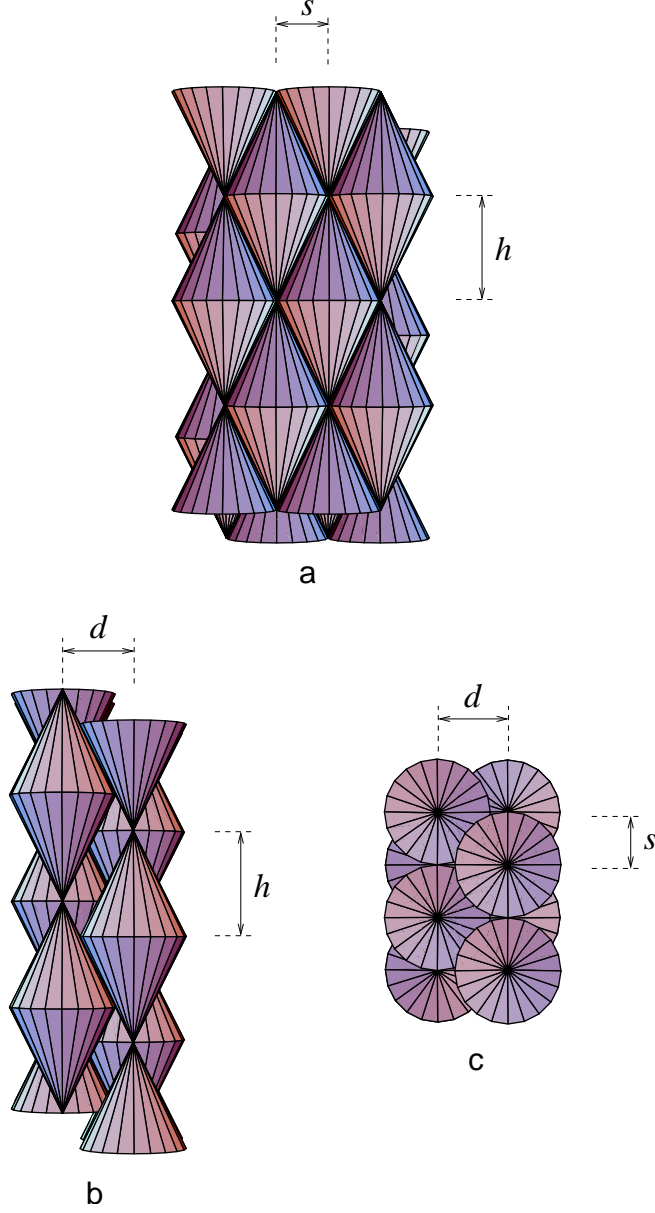


FIG. 2: Stack of planes formed by cones. a), b) and c) are three side views of a stack of two planes shown in Fig. 1(d). In (b), the vertical shift of the first layer with respect to the second layer is  $L \cos(\frac{\alpha}{2})/3$ , where  $L$  is the slant height of the cone and  $\alpha$  is opening angle of the cone at its apex. The layer separation is  $d = \frac{4}{3}L \sin(\frac{\alpha}{2})$ . The lateral shift of successive planes is  $s = L \sin(\frac{\alpha}{2})$ , and the height of the elementary cell is  $h = L \cos(\frac{\alpha}{2})$ .

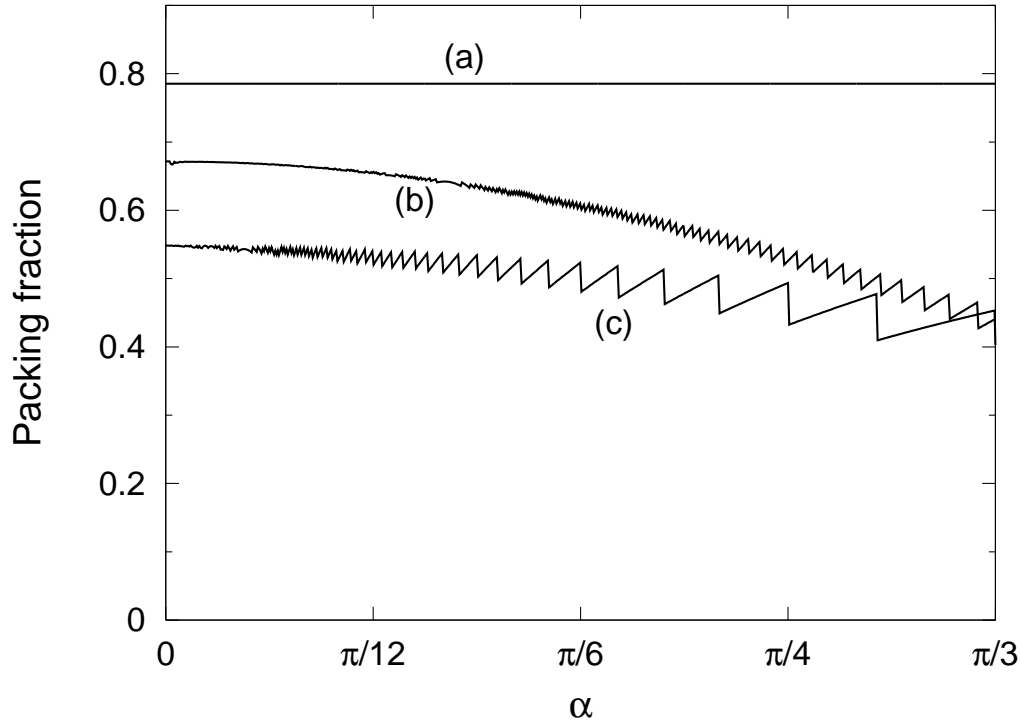


FIG. 3: Dependence of the packing fraction of cones with a flat base on the cone's opening angle at the apex,  $\alpha$ . a) The packing fraction of the stack of planes shown in Fig. 2. This packing fraction is independent of the angle  $\alpha$  and is equal to  $\frac{\pi}{4}$ . b) Packing fraction of a face-centered-cubic lattice of spherical micelles [20] formed by the cones. c) Packing fraction of a hexagonal arrangement of cylindrical micelles [20]. One can show that appropriately stacked planes shown in Fig. 1(e) also yield packing fractions greater than the micellar arrangements.

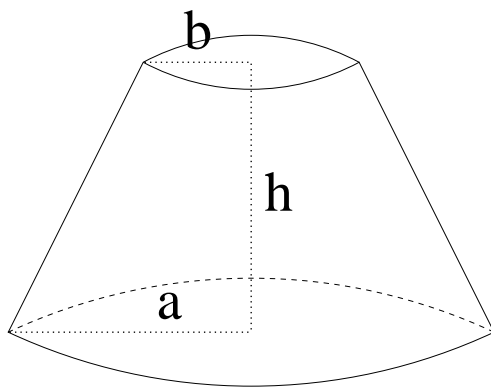


FIG. 4: Conical frustum of height  $h$ , base radius  $a$ , and top radius  $b$  ( $a \geq b$ ).

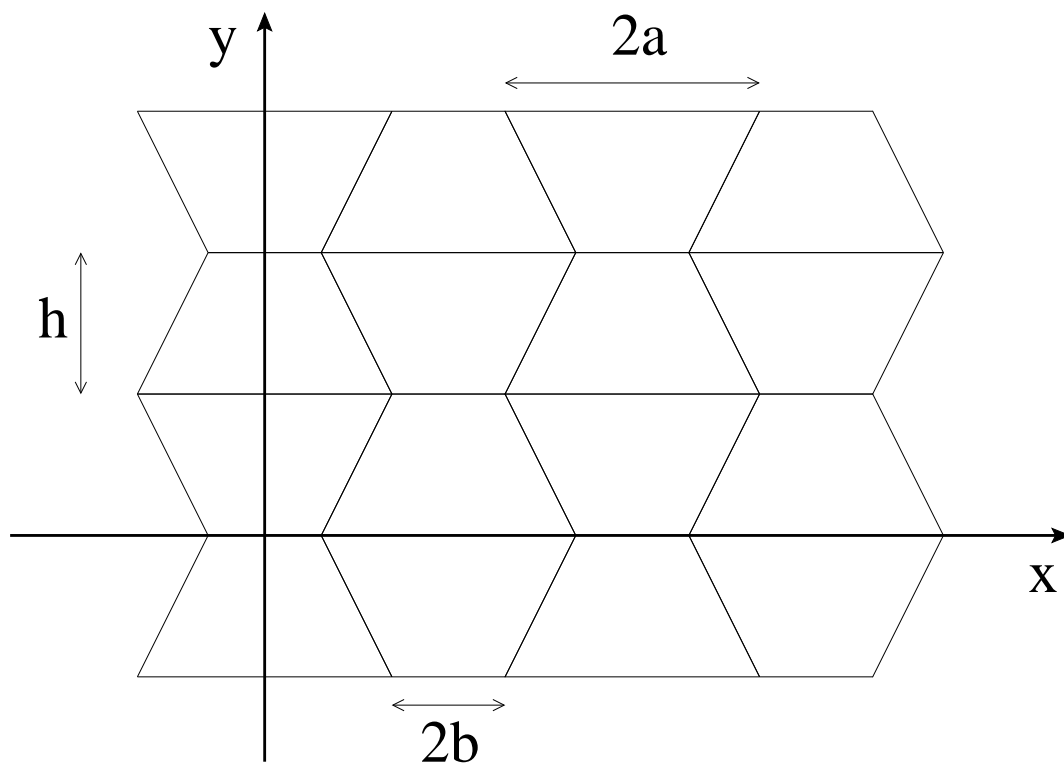


FIG. 5: Close-packed planar layer of truncated cones.

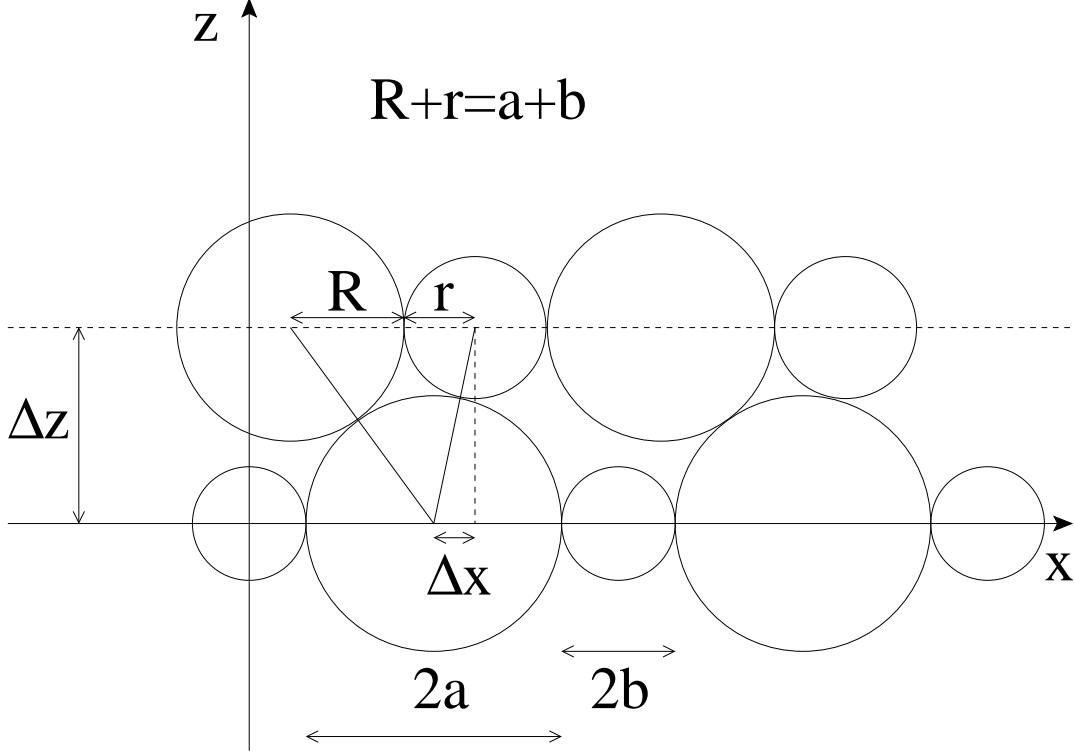


FIG. 6: Intersection of the plane  $y = 0$  with two layers of the stack. The lower circles belong to cones in the first layer ( $z = 0$ ) and are either base or top circles with radius  $a$ ,  $b$ , respectively. The upper circles belong to cones in the second layer ( $z = \Delta z$ ). Their radii  $r$ ,  $R$  ( $b \leq r, R \leq a$ ) are determined by the shift  $\Delta y$  along the  $y$  axis and always fulfill the relation  $R + r = a + b$ . The shifts  $\Delta x$  and  $\Delta z$  between the two layers in the  $(x, z)$  plane are shown. The condition of mutual tangency of the ‘big’ base circle from the first layer with both circles from the second layer is shown.



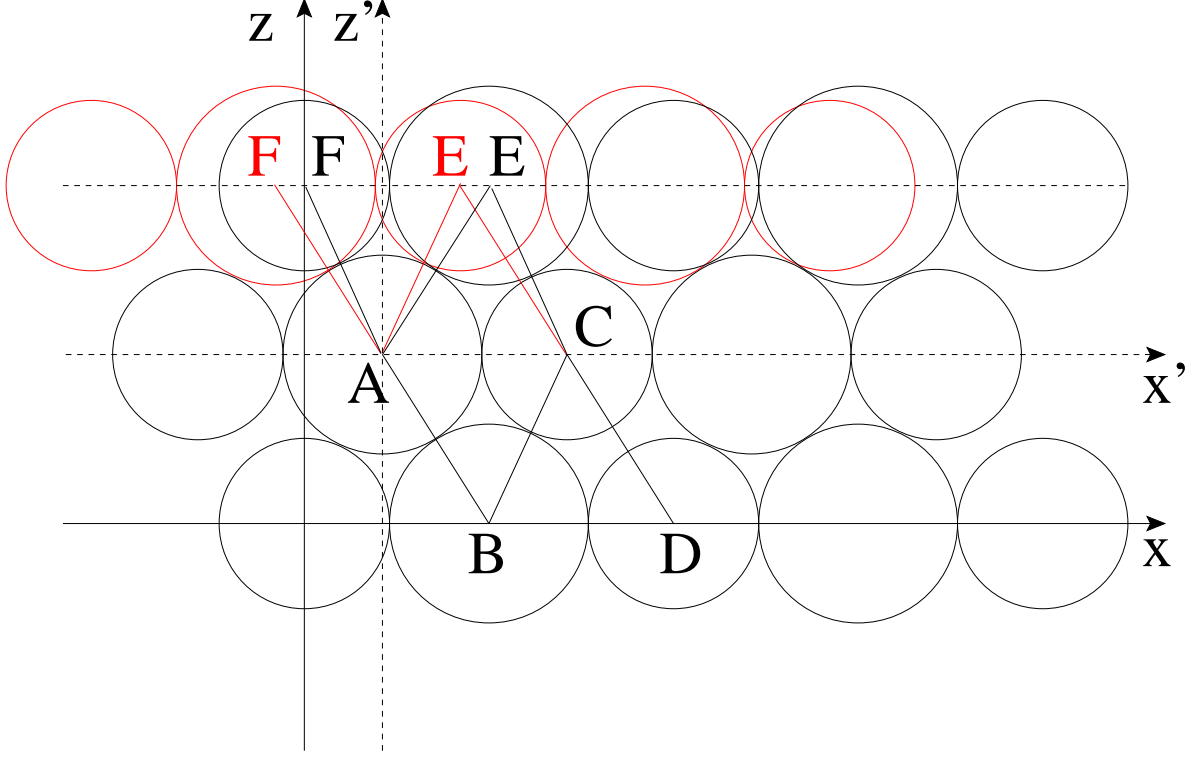


FIG. 7: Intersection of the plane  $y = 0$  with multiple layers of the stack in the cylinder-like regime  $c > c^*$ . Note that  $\Delta x \neq 0$  whereas  $r = a$  and  $R = b$ . The two different ways of adding the third layer to the stack are shown (in black and red). The triangles  $ACB$  and  $BCD$  are isosceles because  $\overline{AC} = \overline{BD} = \overline{BC} = a + b$  whereas  $\overline{AB} = \overline{CD} = 2a$ . For triangle  $ACB$ , all sides pass through tangency points (“full” triangle) whereas the same does not happen for triangle  $BCD$  (“empty” triangle). The choice one has in placing the third layer is equivalent to selecting how to continue the isosceles triangular tiling or equivalently where to place the “empty” triangles. The triangle  $AEC$  is “full” in the black case and “empty” in the red case. Note that in the reference frame  $(x', z')$  defined by the second layer the two possible placements (black and red) of the third layer are related to each other by the reflection  $x' \rightarrow -x'$ . In the cylinder limit,  $c = 1$ , one recovers equilateral triangular tiling, all triangles are “full”, the triangle  $AEF$  remains the same under the reflection  $x' \rightarrow -x'$  and no degeneracy is present anymore. Rotations by  $\pi$  about the  $x$ ,  $y$ , or  $z$  axis relate different stacking variants to each other, showing that the packing of truncated cones in this regime is biaxial [5], with special directions  $x$ ,  $y$ ,  $z$ .

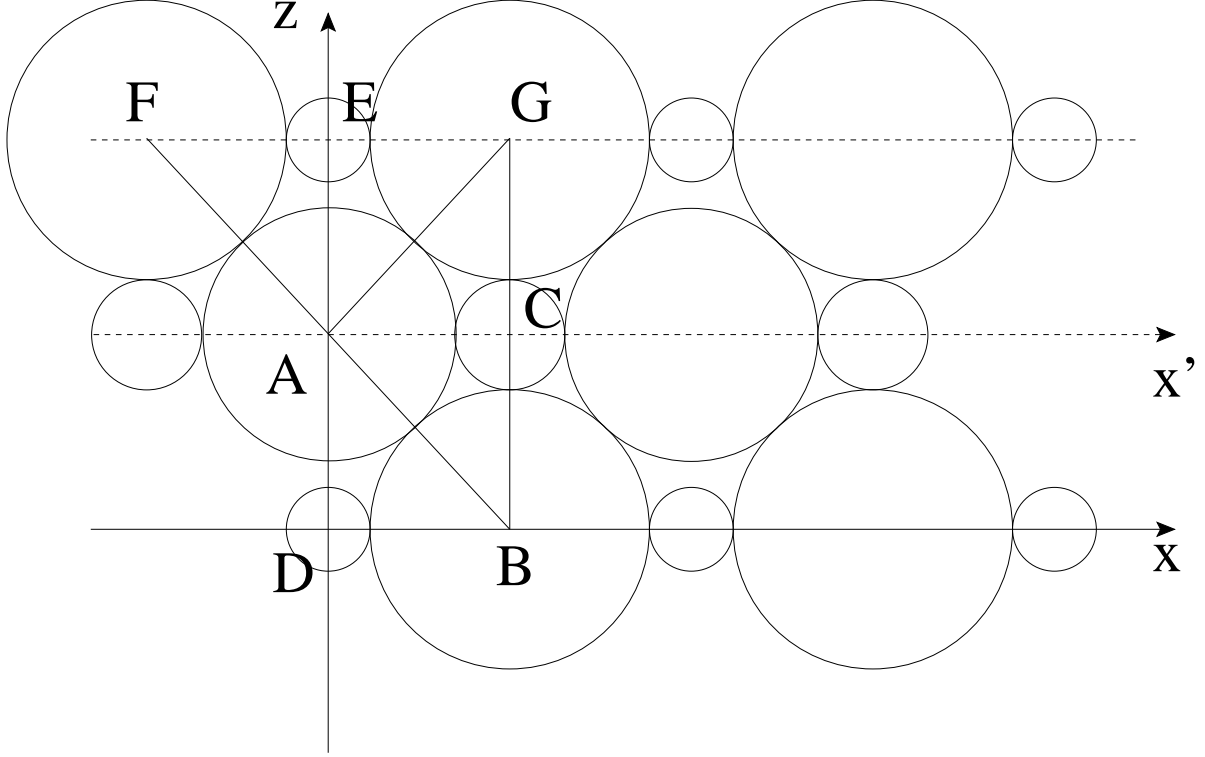


FIG. 8: Intersection of the plane  $y = 0$  with multiple layers of the stack in the cone-like regime  $c < c^*$ . Note that  $\Delta x = 0$  and  $r \neq b$ ,  $r \neq a$ . The triangles  $ACB$  and  $ABD$  are right angled but not isosceles because  $\overline{AC} = \overline{BD} = a + b = r + R$ ,  $\overline{BC} = \overline{AD} = a + r > a + b$ , and  $\overline{AB} = a + R$ . For triangle  $ACB$  all sides pass through tangency points (“full” triangle) whereas the same does not happen for triangle  $ABD$  (“empty” triangle). The triangle  $AEF$  is changed into the equivalent “empty” triangle  $AEG$  under the reflection  $x' \rightarrow -x'$ . The two degenerate solutions are not visible in the  $(x, z)$  plane because they are connected by the reflection  $y' \rightarrow -y'$ . Rotations by  $\pi$  about the  $x$ ,  $y$ , or  $z$  axis relate different stacking variants to each other, showing that the packing of truncated cones in this regime is biaxial [5], with special directions  $x$ ,  $y$ ,  $z$ .

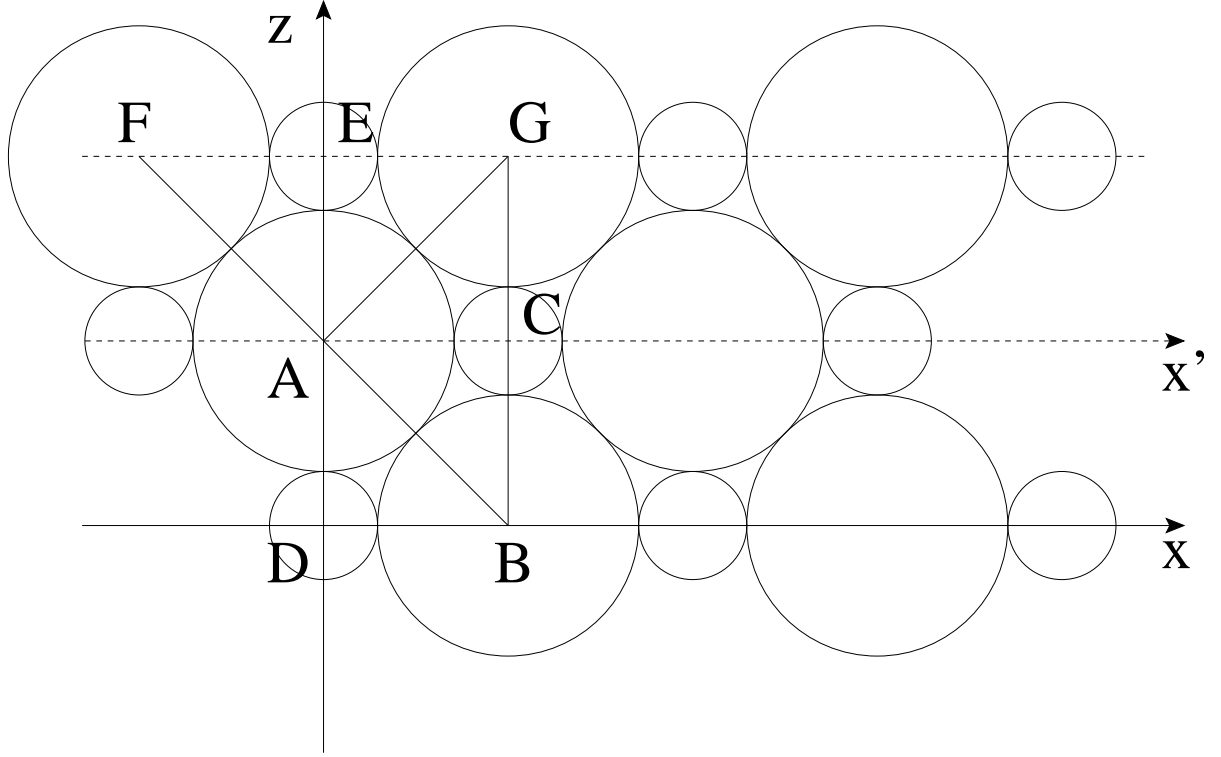


FIG. 9: Intersection of the plane  $y = 0$  with multiple layers of the stack at the transition point  $c = c^*$ . Note that  $\Delta x = 0$  and  $r = b$  ( $\Delta x = a + b$  and  $R = a$  corresponds to the same solution). The triangles  $ACB$  and  $ADB$  are right angled and isosceles because  $\overline{AC} = \overline{BD} = \overline{BC} = \overline{AD} = a + b$ , whereas  $\overline{AB} = 2a$ . For each triangle all sides pass through tangency points, i.e. all triangles are “full”. The triangle  $AEF$  is changed into the equivalent triangle  $AEG$  under reflection  $x' \rightarrow -x'$ , so that no degeneracy is present in this case.

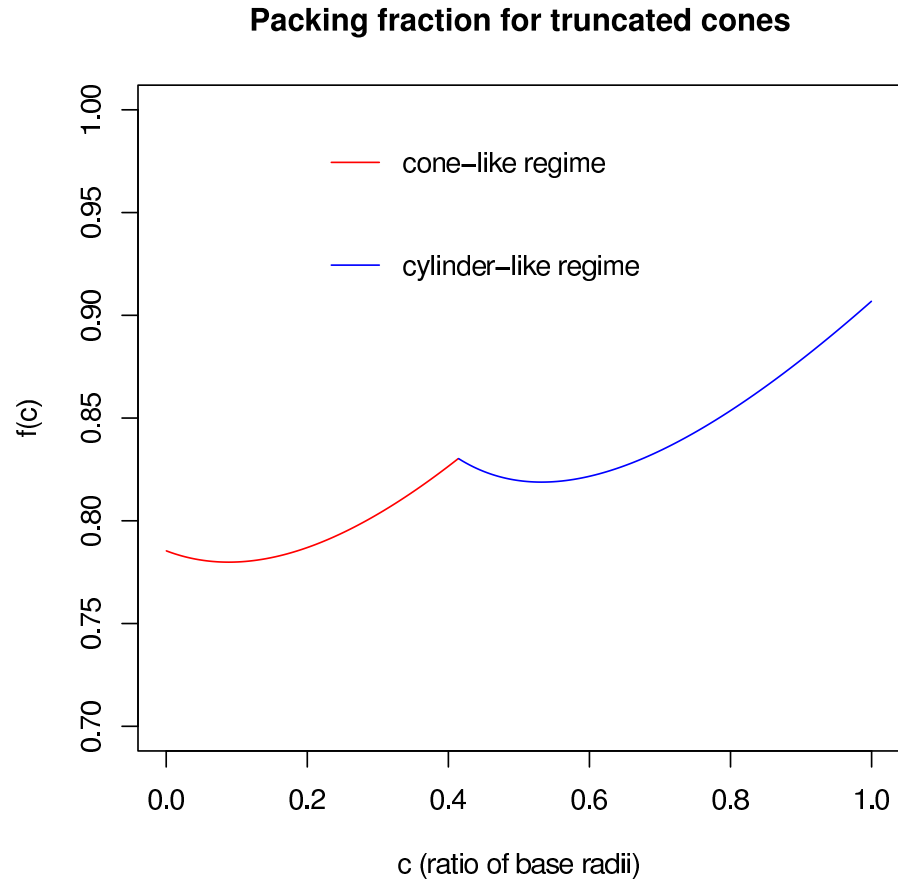


FIG. 10: Packing fraction  $f(c)$  as a function of the base radii ratio  $c$  from equations (5) (red line, cone-like regime) and (6) (blue line, cylinder-like regime).

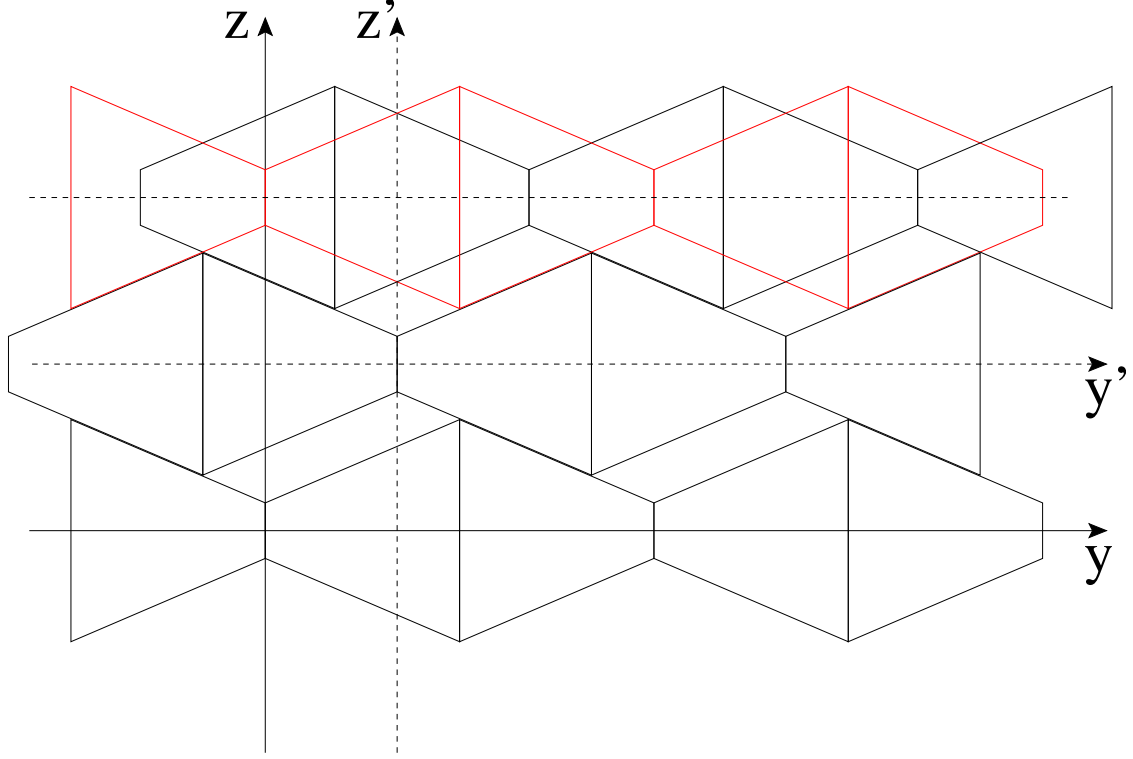


FIG. 11: Intersection of the plane  $x = 0$  with multiple layers of the stack in the cone-like regime  $c < c^*$ . Note that  $\Delta y \neq 0$ . The two different ways of adding the third layer to the stack are shown (in black and red). Note that in the reference frame  $(y', z')$  defined by the second layer, the two possible placements (black and red) of the third layer are related to each other by the reflection  $y' \rightarrow -y'$ . In the cylinder-like and threshold regime  $c \geq c^*$ ,  $\Delta y = 0$  if  $r = a$ , and no void is observed when the packing is viewed in the  $(y, z)$  plane.

## V. SUPPLEMENTARY TEXT

### A. Packing of truncated cones

We wish to study the packing of truncated cones (see Fig. 4). We make the plausible assumption that the best packing can be found by first arranging the truncated cones in a close-packed planar layer, as in Fig. 5 and then stacking consecutive layers on top of each other. A reference frame is attached to each layer, as in Fig. 5, so that the shift between consecutive layers in the stacking is defined as the shift  $(\Delta x, \Delta y, \Delta z)$  between the origins of the corresponding frames. Rotations (along the  $z$  axis) can be defined similarly, but we assume that the rotation of a layer with respect to an adjacent one in the stacking leads to a worse packing.

The results presented in the following are obtained by finding the values of  $\Delta x$  and  $\Delta y$  that minimize  $\Delta z$  compatibly with steric constraints (in *Cone Packing* under *Results and Discussion*, the “lateral shift”  $s$  is  $\Delta x$ , the “vertical shift” is  $\Delta y$ , and the layer separation  $d$  is  $\Delta z$ ).

In Fig. 6, the intersection of the plane  $y = 0$  with two layers of the stack is plotted for a generic shift  $\Delta y$  along the  $y$  axis. The radii  $R, r$ , of the resulting circles cut from the cones in the second layer are determined by  $\Delta y$ :

$$R = b + \frac{\Delta y}{h} (a - b) \quad r = a - \frac{\Delta y}{h} (a - b) \quad (8)$$

For any given  $\Delta y$  and  $\Delta x$ , the minimum  $\Delta z$  is obtained by first imposing the condition of double tangency of the ‘big’ base circle from the first layer with both circles from the second layer. The double tangency (already shown to occur in Fig. 6) implies that  $\Delta x$  and  $\Delta z$  are determined as a function of  $\Delta y$ , or alternatively of  $r$  (see Eq. 8).

$$\Delta x = -a + r \frac{3a + b}{a + b} \quad (9)$$

$$(\Delta z)^2 = 4ra(a + b - r) \frac{2a + b}{(a + b)^2} . \quad (10)$$

$(\Delta z)^2$  is then minimized with respect to  $r$ .

Noting that the solutions need to satisfy  $0 \leq \Delta x \leq a + b$  and  $b \leq r \leq a$  (i.e.,  $0 \leq \Delta y \leq h$ ), one gets two different regimes for the optimal stacking depending on the ratio  $b/a$ . Note

that there is a combined periodicity in the  $(x, y)$  plane so that  $\Delta x = 0, r = a$  ( $\Delta y = 0$ ) is the same as  $\Delta x = a + b, r = b$  ( $\Delta y = h$ ).

The optimal stacking depends on the value of the ratio  $c = b/a$ . There is a special transition point  $c^* = \sqrt{2} - 1$  separating two distinct regimes according to whether  $c < c^*$  or  $c > c^*$ . In general, one finds two different degenerate (i.e., yielding the same minimum  $\Delta z$ ) solutions: one for  $r < R$  and one for  $r > R$ . They can be thought to be related by a mirror symmetry  $x \rightarrow -x; y \rightarrow -y$  applied to the second layer while keeping the first layer fixed. This choice among two possibilities has to be taken each time a new layer is added to the stack implying an infinite degeneracy in the close-packing arrangements of cones stacked in planar layers.

### 1. Cylinder-like case

If  $c > c^*$  we are close to the cylinder  $c = 1$  case.

The two solutions are

$$r_1 = b; \quad \Delta x_1 = \frac{b^2 + 2ab - a^2}{a + b}; \quad \Delta y_1 = h \quad (11)$$

$$r_2 = a; \quad \Delta x_2 = \frac{2a^2}{a + b}; \quad \Delta y_2 = 0 \quad (12)$$

yielding

$$\Delta z = \frac{2a}{a + b} \sqrt{b(2a + b)} \quad (13)$$

and a packing fraction ( $F = V_{tc}/V_{\text{cell}}$ , where  $V_{\text{cell}} = h\Delta z(a + b)$  is the volume of the elementary cell in the periodic arrangement of cones and  $V_{tc} = (\pi h/3)(a^2 + ab + b^2)$  is the volume of the truncated cone)

$$F = \frac{\pi}{6} \frac{a^2 + ab + b^2}{a\sqrt{b(2a + b)}}. \quad (14)$$

In this regime, the only effective mirror symmetry is  $x \rightarrow -x$ , since  $\Delta y = h$  or  $\Delta y = 0$ .

In the limiting case of a cylinder ( $a = b$ ), we correctly get

$$r_1 = r_2 = a; \quad \Delta y_1 = \Delta y_2 = 0; \quad \Delta x_1 = \Delta x_2 = a; \quad \Delta z = \sqrt{3}a; \quad F = \frac{\pi}{2\sqrt{3}} = 0.9069 \dots \quad (15)$$

## 2. Cone-like case

If  $c < c^*$ , we are close to the nontruncated cone  $c = 0$  case.

The two solutions are

$$r_1 = \frac{a(a+b)}{3a+b}; \quad \Delta x_1 = 0 \quad (16)$$

$$r_2 = \frac{(a+b)(2a+b)}{3a+b}; \quad \Delta x_2 = a+b \quad (17)$$

yielding

$$\Delta z = \frac{2a(2a+b)}{3a+b}, \quad F = \frac{\pi(3a+b)(a^2+ab+b^2)}{6a(a+b)(2a+b)}. \quad (18)$$

In this regime the only effective mirror symmetry is  $y \rightarrow -y$ , since  $\Delta x = a+b$  or  $\Delta x = 0$  (see Figs. 8 and 11).

In the limiting case of a nontruncated cone ( $b = 0$ ), we correctly get

$$r_1 = a/3, r_2 = 2a/3; \quad \Delta x_1 = 0, \Delta x_2 = a; \quad (19)$$

$$\Delta y_1 = 2h/3, \Delta y_2 = h/3; \quad \Delta z = 4a/3; \quad F = \frac{\pi}{4} = 0.7854 \dots \quad (20)$$

and we recover the result in *Cone Packing* under *Results and Discussion*.



### 3. *Threshold case*

The special value  $c = c^*$ , i.e.,  $b = (\sqrt{2} - 1)a$ , separates the two regimes.

The two solutions are

$$r_1 = b; \quad \Delta x_1 = 0; \quad \Delta y_1 = h \quad (21)$$

$$r_2 = a; \quad \Delta x_2 = a + b; \quad \Delta y_2 = 0 \quad (22)$$

yielding

$$\Delta z = \sqrt{2}a, \quad F = \frac{\pi}{6} (3 - \sqrt{2}) = 0.8303 \dots \quad (23)$$